

COMMUNICATION

On-Demand Nanozyme Signal Enhancement at the Push of a Button for the Improved Detection of SARS-CoV-2 Nucleocapsid Protein in Serum

Received 00th January 20xx,
Accepted 00th January 20xx

DOI: 10.1039/x0xx00000x

Daniel W. Bradbury,^a Jasmine T. Trinh,^a Milo J. Ryan,^a Cassandra M. Cantu,^a Jiakun Lu,^a Frances D. Nicklen,^a Yushen Du,^{b,c} Ren Sun,^{b,d} Benjamin M. Wu,^{a,e} and Daniel T. Kamei ^{a*}

We developed an innovative 3D printed casing that incorporates a lateral-flow immunoassay, dehydrated signal enhancement reagents, and a sealed buffer chamber. With only the push of a button for signal enhancement, our device detected the SARS-CoV-2 N-protein in 40 min at concentrations as low as 0.1 ng/mL in undiluted serum.

1. Introduction

The severe acute respiratory syndrome coronavirus 2 (SARS-CoV-2) has caused an ongoing and devastating pandemic which remains a major threat to global public health.^{1,2} The nucleocapsid protein (N-protein) is a major structural protein of coronaviruses which is involved in the packing of RNA within the virus. It is highly conserved between coronaviruses, with the SARS-CoV and SARS-CoV-2 N-proteins sharing 90% homology.³ During the first week of infection, the N-protein is shed at relatively high concentrations into nasopharyngeal fluid and serum.⁴ It has previously been utilized to diagnose SARS-CoV infections, where the viral N-protein could be detected as early as 1 day after onset of symptoms in a variety of different bodily fluids.⁵ Recent studies have shown that patients in the early stages of infection with SARS-CoV-2 also have detectable circulating N-protein in serum.^{6,7} Due to its functional significance to coronaviruses and its abundance in bodily fluids,

it has been suggested that the N-protein in serum could serve as an antigen target for early SARS-CoV-2 detection.

An at-home diagnostic would allow for more widespread rapid detection of initial infection in a low-cost manner, which would allow patients to be treated and quarantined to prevent further outbreaks. This is especially important as the current gold standard for detecting SARS-CoV-2 is reverse transcription real-time PCR, which requires samples to be sent to laboratories that have equipment, power, and trained personnel. This leads to a delay in the individual receiving results and therefore potential for continued transmission of the virus.⁸ Lateral-flow immunoassays (LFAs) exhibit many of the characteristics desired for point-of-care diagnostics and can easily be performed at home with the correct sampling method. The most common application of LFAs is the over-the-counter pregnancy test. Having a similar rapid, inexpensive, and easy-to-use test for SARS-CoV-2 will lead to widespread screening of healthy, asymptomatic, and symptomatic individuals. This blanket screening approach will play a significant role in allowing society to return to normal while maintaining safety.

Several LFAs that directly detect the spike protein and N-protein within the first week of infection have become commercially available during the pandemic through the FDA's Emergency Use Authorization.⁹⁻¹¹ It is important to note that all of the antigen-based LFAs currently available use nasal and/or nasopharyngeal swabs for sample collection. While the use of a nasopharyngeal swab has greater potential to sample and capture virus due to the localization of SARS-CoV-2 in the upper respiratory tract, it requires some level of guidance to ensure proper sample collection and thus is not ideal for at-home testing. Both swabbing collection methods are also prone to user error and variation depending on how the user inserts the swab into the nasal cavity. In fact, swabbing variability has been shown to impact even highly sensitive laboratory diagnostics for SARS-CoV-2.^{12,13} Additionally, nasal and nasopharyngeal swabs must be significantly diluted into a buffer before being utilized in any LFA-based diagnostic. These disadvantages cause the

^a Department of Bioengineering, University of California, Los Angeles, CA 90095 USA

Email: kamei@seas.ucla.edu

^b Department of Molecular and Medical Pharmacology, University of California, Los Angeles, CA 90095 USA

^c ZJU-UCLA Joint Center for Medical Education and Research, Collaborative Innovation Center for Diagnosis and Treatment of Infectious Diseases, Cancer Institute, The Second Affiliated Hospital, Zhejiang University School of Medicine, Hangzhou 310058, China

^d School of Biomedical Sciences, Li Ka Shing Faculty of Medicine, The University of Hong Kong, Hong Kong, China

^e Division of Advanced Prosthodontics & Weintraub Center for Reconstructive Biotechnology, School of Dentistry, University of California, Los Angeles, CA 90095 USA

nasal and nasopharyngeal swabs to be less-than-ideal sample collection methods for an at-home diagnostic.

In contrast, sample fluids such as blood, serum, and saliva can be utilized and are easier to collect consistently. However, they cannot be used with the currently available LFA technology due to having lower viral loads or antigen concentrations than those in nasopharyngeal samples. Li and Lillejoh recently reported the development of the first smartphone-based, microfluidic point-of-care device for the sensitive quantification of N-protein in serum down to 0.1 ng/mL. While able to detect low levels of N-protein, this assay requires the user to perform multiple reagent addition steps and possess a smartphone, potentially limiting its applicability for self-testing and widespread use in low resource regions.¹⁴ An alternative approach is to develop a more sensitive version of the LFA which maintains its ease-of-use and equipment-free characteristics while also being able to detect low levels of N-protein in blood. Some common techniques to improve LFA sensitivity involve biomarker preconcentration and signal enhancement.^{15,16}

While gold nanoparticles are the most widely used detection probes for LFAs, other probes such as magnetic nanoparticles, carbon nanoparticles, quantum dots, luminescent nanoparticles, and colored latex have been used to improve sensitivity or provide additional functionalities.^{17–22} In this work, we use platinum-coated gold nanzymes (PtGNPs) for their demonstrated ability to exhibit peroxidase-like activity at acidic pH levels.²³ Previously, our lab has used this peroxidase-like activity to introduce a purple 3,3',5,5'-tetramethylbenzidine (TMB) precipitate to enhance the LFA signal.¹⁶ For this device, the reagents required for this process are dehydrated to make them more suitable for an at-home test.

In this work, we developed a novel paper-based device that incorporates an LFA test strip, dehydrated signal enhancement reagents (nanzymes and their associated chemicals), and a sealed chamber with stored liquid enhancement buffer in an innovative 3D printed casing. Our device enabled the detection of N-protein in undiluted serum in 40 min at concentrations as low as 0.1 ng/mL, which was at least a 10-fold improvement over the conventional LFA. Moreover, with this all-in-one device, only one simple step of pushing a single button is needed for the signal enhancement to occur after the LFA detection step.

2. Materials and Methods

2.1 Preparation of biotinylated anti-N-protein capture antibodies

All reagents and materials were purchased from Sigma-Aldrich (St. Louis, MO) unless otherwise noted. Biotinylated anti-N-protein capture antibodies were prepared by NHS-ester linkage using NHS-PEG-biotin. 15 μ L of a 3 mM NHS-PEG-biotin solution was added to 50 μ L of 0.5 mg/mL anti-N-protein antibodies (#40143-MM05, Sino Biological, Wayne, PA) in phosphate-buffered saline (PBS, pH 7.4) and reacted for 30 min, allowing the NHS-PEG-biotin to conjugate onto the free surface primary amines of the antibodies. The conjugation reaction was stopped

via buffer exchange in fresh PBS using Zeba Spin Desalting Columns (Fisher Scientific, Waltham, MA).

2.2 Preparation of anti-N-protein detection antibody decorated platinum-coated gold nanzyme probes (anti-N-protein PtGNPs)

Platinum-coated gold nanzymes were synthesized using a protocol derived from Gao et al.²³ Briefly, 4 mL of 40 nm citrate-capped gold nanoparticles (GNs) (Nanocomposix, San Diego, CA) and 1686 μ L of filtered ultrapure water were preheated to 90°C in an oil bath under magnetic stirring for 20 min. Following the preheating, 314 μ L of a 0.82 mM chloroplatinic acid hydrate solution and 2 mL of a 3.3 mM ascorbic acid solution were injected separately into the gold nanoparticle suspension using a syringe pump at rates of 0.6 and 1.2 mL/h, respectively. The reaction was allowed to proceed for 1 h after the injection was complete.

To create anti-N-protein decorated platinum-coated gold nanzyme probes (anti-N-protein PtGNPs), 30 μ L of a 0.1 M sodium borate solution (pH 9) was first added to 1 mL of PtGNPs. Then, 4 μ g of primary anti-N-protein antibody (#40143-R001, Sino Biological, Wayne, PA) was added to the suspension and incubated for 30 min at room temperature (22°C). 50 μ L of a 10% (w/v) bovine serum albumin (BSA) in filtered ultrapure water solution was then added to the suspension and incubated for 10 min. Free antibodies were removed with three centrifugation cycles at 8600 RCF and 4°C for 6 min each. For the first two cycles, the pellet was resuspended in 200 μ L of 1% (w/v) BSA in filtered ultrapure water, and the final pellet was resuspended to a final volume of 50 μ L in 0.1 M sodium citrate buffer (pH 6).

2.3 Preparation of LFA test strip

The LFA test strips were composed of overlapping pads secured to an adhesive backing. These pads included a biotinylated-anti-N-protein antibody pad, an anti-N-protein PtGPN conjugate pad, a nitrocellulose membrane, and a CF4 absorbent pad (Cytiva, Marlborough, MA). To prepare the detection region of the LFA, proteins were first printed and immobilized on a Unisart CN140 nitrocellulose membrane (Sartorius, Göttingen, Germany) using an Automated Lateral Flow Reagent Dispenser (Claremont BioSolutions LLC, Upland, CA) with the voltage setting at 4.5 V and a Fusion 200 syringe pump (Chemex Inc, Stafford, TX) with a flow rate of 300 μ L/min. The test line was formed by printing a solution of a 2 mg/mL polystreptavidin (Biotez, Berlin, Germany) solution in 25% (w/v) sucrose. The control line was formed by printing a solution of 0.25 mg/mL goat anti-rabbit IgG secondary antibody in 25% (w/v) sucrose. The printed membrane was left in a vacuum-sealed desiccator overnight and subsequently stored in a bag containing Drierite desiccant (W.A. Hammond Drierite Co, Xenia, OH) for an additional day.

To create each nanzyme conjugate pad, 6 μ L of anti-N-protein PtGNPs were diluted to form a 20 μ L solution with final concentrations of 5% (w/v) trehalose and 1% (w/v) BSA and then dehydrated onto a 5 mm \times 10 mm piece of Standard 17 fiberglass paper (Cytiva, Marlborough, MA). The conjugate pads

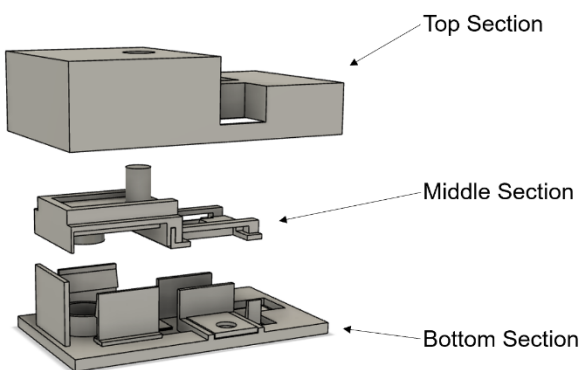


Fig. 1 Design of the three main casing pieces for nanozyme signal enhancement of the LFA.

were dehydrated in a desiccator at 37°C overnight. To create each capture antibody pad, 2 μ L of a 0.05 mg/mL biotinylated anti-N-protein capture antibody solution was diluted to form a 20 μ L solution with final concentrations of 5.74% (w/v) trehalose and 1.15% (w/v) BSA and then dehydrated onto a 5 mm \times 10 mm piece of fiberglass paper. The pads were dehydrated in a vacuum-sealed desiccator overnight.

To assemble the LFA test strip, the nitrocellulose membrane was first adhered to an adhesive backing. Individual strips were cut to be 5 mm in width. To each strip, a CF4 absorbent pad was placed on the adhesive backing downstream of the control line, overlapping the nitrocellulose membrane by 3 mm. The PtGNP conjugate pad was placed on the adhesive backing upstream of the test line, overlapping the nitrocellulose membrane by 2 mm. The biotinylated capture antibody pad was placed on the adhesive backing upstream of and overlapping the PtGNP conjugate pad by 1 mm.

2.4 Design and assembly of device for enhancement reagent storage and delivery on LFA

A casing was designed to eliminate the need for multiple liquid and test strip-handling steps. This 3D printed device provides in-test liquid reagent storage, dehydrated enhancement reagents, and movable paper architecture that directs the flow of liquid

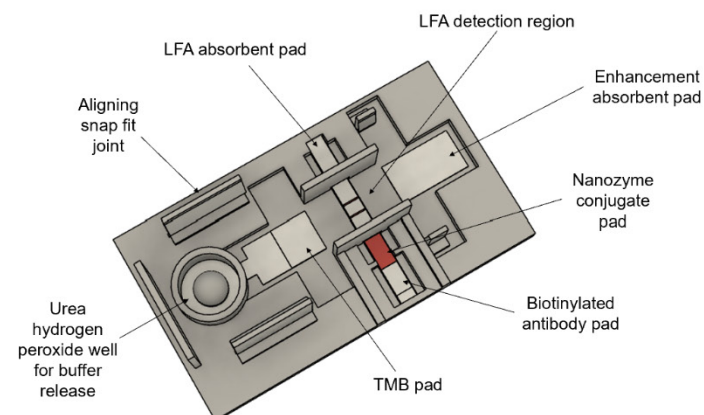
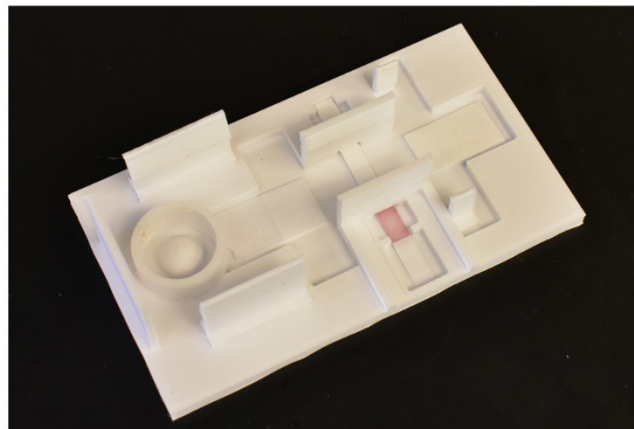


Fig. 2 (Left) Labelled CAD drawing of bottom piece of casing. (Right) Photograph of 3D printed bottom piece of casing with LFA test strip and enhancement reagent paper pads in position.

through the LFA test strips. The three major components of the device are outlined in **Fig. 1**. The parts shown in gray were 3D printed using an Ultimaker 3 FDM 3D printer (Ultimaker B.V., Geldermalsen, Netherlands) out of Ultimaker CPE filament (co-polyester).

The bottom piece of the casing, along with the inserted paper pads and test strip, are detailed in **Fig. 2**. The enhancement buffer release well is an enclosed, hollow cylinder with a dome in the center. The dome serves to rupture a foil sealed buffer reservoir on the middle piece of the casing. 0.05 g of urea hydrogen peroxide was sprinkled in the hollow cylinder surrounding the dome and then covered with a ring of fiberglass paper. A 62.5 μ L solution of 6.5 mM TMB, 15% (w/v) trehalose, and 20% (w/v) dimethylformamide in 0.1 M sodium citrate buffer (pH 5) was dehydrated onto a 13 mm \times 12 mm fiberglass pad overnight in a vacuum sealed desiccator to create the TMB pad. The enhancement reagent absorbent pad is composed of a 13 mm \times 23 mm CF4 absorbent pad. The four aligning snap fit joints hold the middle piece of the casing in a lifted position until the user presses down on it. When pressed, the middle piece then snaps into place and is held down in a constant position by the snap fit joints. The bottom piece also contains a sample well which is located above the biotinylated capture antibody pad when the device is fully assembled.

The movable middle piece of the casing, shown in **Fig. 3**, contains the enhancement buffer reservoir and two connector pads. The left pad is made up of Standard 17 fiberglass paper while the right pad is a CF4 absorbent pad. The enhancement buffer, which will solubilize the urea hydrogen peroxide and TMB during the assay, was stored within the reservoir of the middle piece. To fill the reservoir, 600 μ L of 1% (w/v) dextran sulfate in 0.1 M sodium citrate buffer (pH 5) was pipetted into the reservoir. To seal the liquid in the reservoir, a sheet of mylar foil was placed on top of the reservoir and heat was applied using a hot iron for 3 s followed by complete cooling. The top piece of the casing serves to help hold the other components in place and protect them from external and environmental factors. It also contains a viewing window to observe the detection results (**Fig. 4A**).



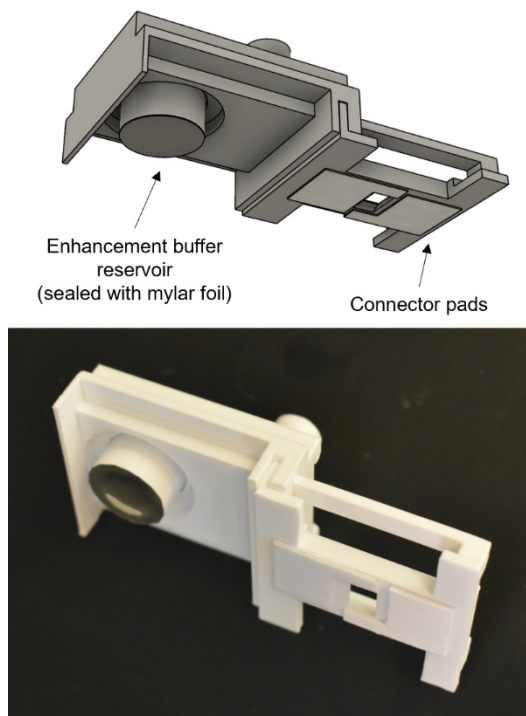


Fig. 3 CAD drawing (top) and 3D printed piece (bottom) showing the underside view of the middle piece of the casing and the locations of the enhancement buffer fluid reservoir and the paper connector pads.

2.6 Detection of N-protein in human serum with nanozyme signal enhanced LFA

To detect for N-protein using our nanozyme signal enhanced LFA, a 25 μ L human serum sample (#50-203-6415, Fisher Scientific, Waltham, MA) spiked with varying concentrations of N-protein (#40588, Sino Biological, Wayne, PA) was added to the sample well on the LFA (above the biotinylated capture antibody pad). As in the case of typical LFAs for serum samples, this was immediately followed by a chase buffer. In our system, we used 75 μ L of chase buffer composed of 2% (w/v) polyvinylpyrrolidone 10kDa, 0.2% (w/v) BSA, 0.2% (w/v) Tween 20, and 0.2% (w/v) casein in 0.1 M potassium phosphate at pH

7.2. After 20 min, the user pressed the button to move down the middle piece of the casing (**Fig. 4B**). The movement of the middle casing piece resulted in the rupture of the mylar seal to release the enhancement buffer and also served to lower the connector pads to provide a continuous flow path for the enhancement reagents to flow through the LFA strip. Final results were observed after 20 min of enhancement. Results were photographed before and after the signal enhancement reaction with a Nikon D3400 digital camera (Nikon, Tokyo, Japan) in a controlled lighting environment. To quantify the relative test line intensities, the resulting images were processed by a MATLAB script developed by our lab.²⁴

2.7 Cross-reactivity tests with other N-proteins

To test for cross-reactivity of our device with the Middle East respiratory syndrome coronavirus (MERS-CoV) N-protein (#40068, Sino Biological, Wayne, PA) and human coronavirus 229E (HCoV-229E) N-protein (#40640, Sino Biological, Wayne, PA), the assay was run using the same steps as described in Section 2.6. Samples of SARS-CoV-2 N-protein, MERS-CoV N-protein, and HCoV-229E N-protein were tested at 1.0 ng/mL in human serum.

3. Results and Discussion

3.1 Demonstration of improved N-protein detection using nanozyme signal enhancement

The operation of our device for the nanozyme signal enhanced detection of N-protein occurs in two main steps. The first is the antigen capture and detection step and the second is the signal enhancement step (**Fig. 5**). The user first applies the serum sample to the sample well immediately followed by the addition of the chase buffer. The liquid will first resolubilize the biotinylated capture anti-N-protein antibody and then the anti-N-protein PtGNPs. In the case of a positive sample, these antibody species will bind to any N-protein in the sample resulting in the formation of sandwich complexes. As these complexes flow through the LFA strip, they will be captured at the test line due to the strong biotin-streptavidin interaction

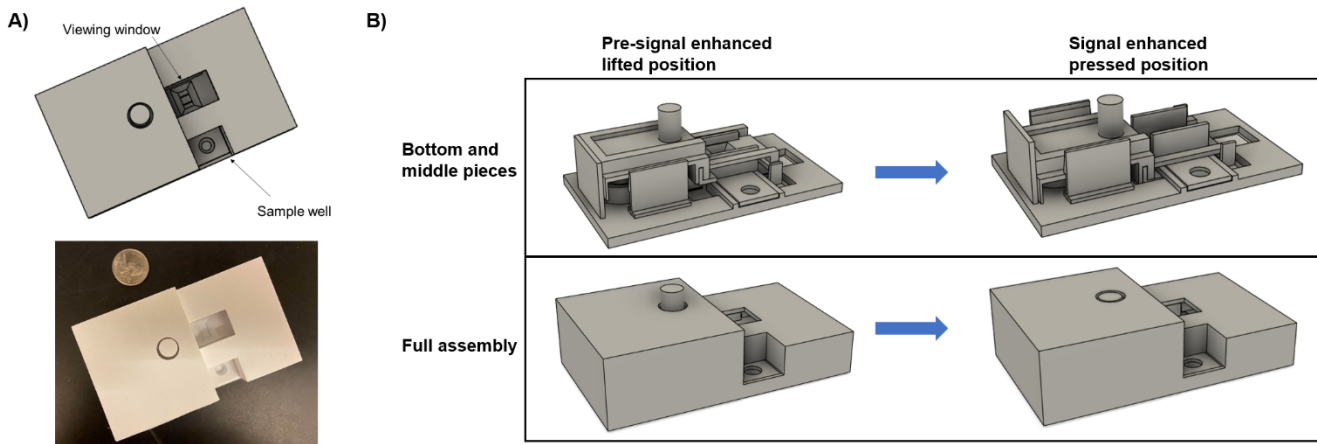


Fig. 4 **(A)** CAD drawing (top) and 3D printed (bottom) full casing assembly with labelled viewing window and sample well. US quarter included for size comparison. **(B)** CAD drawings showing the casing before and after pressing the middle piece.

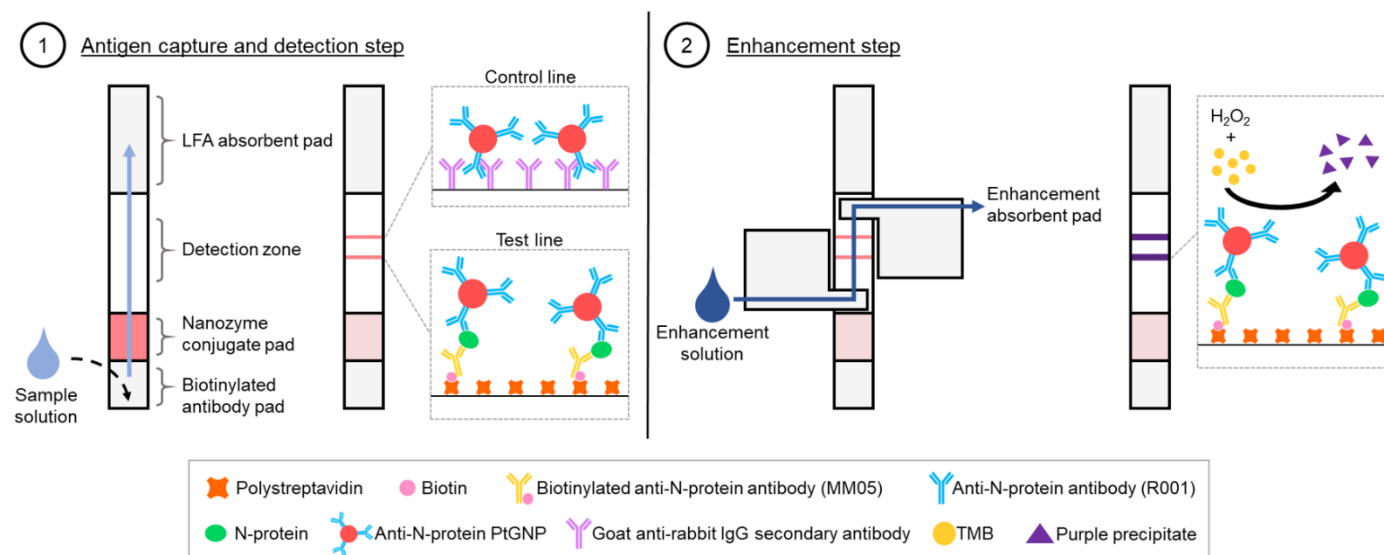


Fig. 5 Simplified schematic of assay steps and paper segments touching the LFA test strip. (1) Sample is applied to the sample well above the test strip where biotinylated antibody and PtGNPs are rehydrated and antigen capture occurs at the detection zone. (2) After pressing the button to move the middle piece of the casing down, enhancement buffer is released to rehydrate the dehydrated enhancement reagents and flow through the test strip resulting in signal enhancement at the detection zone.

between the biotinylated capture antibody and the streptavidin immobilized on the test line. This will ultimately result in the capture of PtGNPs at the test line region. In the case of a negative sample where no N-protein is present, no sandwich complex will form. Therefore, even though the biotinylated capture antibody will bind to the streptavidin at the test line, no PtGNPs will be captured. Regardless of the sample being positive or negative for N-protein, any PtGNPs that do not get captured at the test line will be able to be captured by the secondary antibody at the control line to indicate that the sample flowed properly through the test strip.

After 20 min, instead of the typical signal enhancement process of a user creating a signal enhancement solution and then physically moving the LFA strip into that solution, the user will only need to press down on the button connected to the middle piece of the casing. This lowers the middle piece where it snaps into place with the connector pads bridging gaps between the dehydrated TMB pad and the LFA strip, as well as the LFA strip and the enhancement absorbent pad. Additionally, as the middle piece is lowered, the mylar seal on the enhancement buffer reservoir is ruptured by the dome, which

allows the enhancement buffer to flow into the release well. Once released, the buffer solubilizes the urea hydrogen peroxide, followed by the TMB. This enhancement solution then flows through the LFA test strip and into the enhancement absorbent pad. As the solution passes the detection zone, any PtGNPs bound to the test line will catalyze the oxidation of TMB to TMB^+ . The TMB^+ will complex with the negatively charged dextran sulfate, leading to the formation of an insoluble purple product that becomes deposited at the test line. This results in the enhancement of the test line signal over an additional 20 min, improving the sensitivity of the LFA.

To evaluate the performance of this assay, we tested samples containing 0, 0.03, 0.1, 0.3 and 1 ng/mL of N-protein spiked into human serum. The final LFA strips from one of our experimental studies are shown in **Fig. 6**. Before the enhancement step, a clearly visible test line is present at 1 ng/mL but not at 0.3 ng/mL, indicating a detection limit of 1

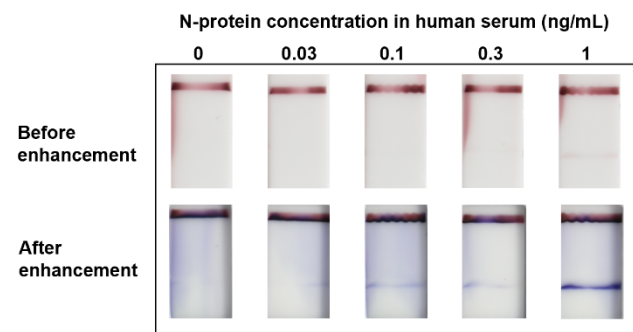


Fig. 6 Detection of the N-protein of SARS-CoV-2 in human serum using nanozyme signal enhanced LFA. Detection limit before enhancement is 1 ng/mL while after enhancement it is 0.1 ng/mL, demonstrating at least a 10-fold improvement in detection limit and detection of N-protein within the desired concentration range.

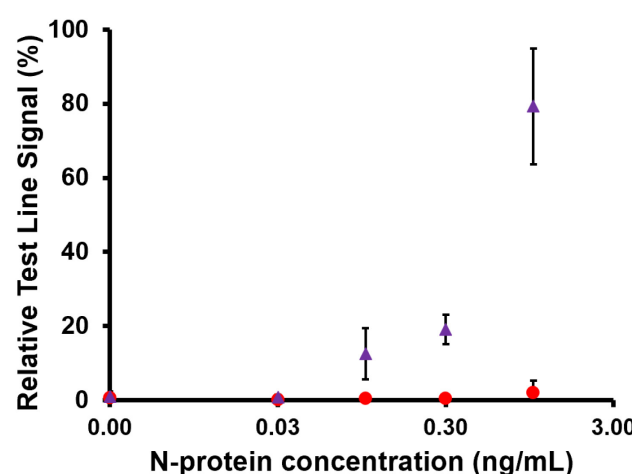


Fig. 7 Plot of relative test line signal intensity versus N-protein concentration for both the LFA (red ●) and enhancement steps (purple ▲). Data is represented as the mean \pm SD ($n = 4$).

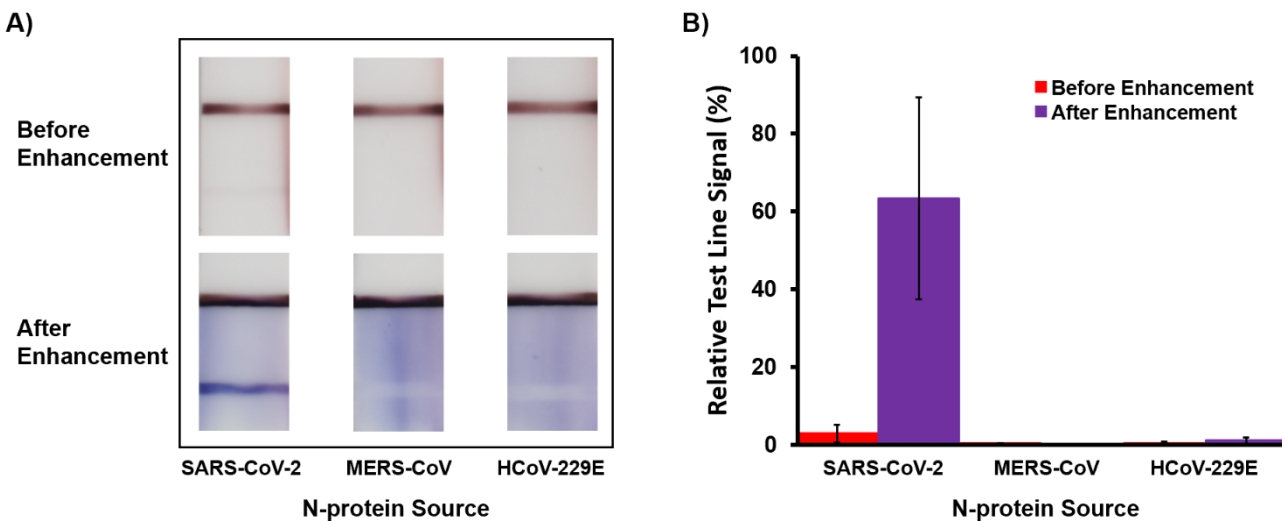


Fig. 8 (A) Results from cross-reactivity tests with MERS-CoV and HCoV-229E N-proteins, confirming that our assay has no cross-reactivity with the N-proteins from these viruses. Each N-protein was run at 1.0 ng/mL in human serum. (B) Plot of relative test line signal intensity for N-proteins from SARS-CoV-2, MERS-CoV, and HCoV-229E at 1.0 ng/mL in human serum. Data is represented as the mean \pm SD ($n = 3$).

ng/mL. After enhancement, the test line at 1 ng/mL becomes significantly darker and a visible test line also appears at 0.1 and 0.3 ng/mL, demonstrating at least a 10-fold improvement in detection limit.

This experimental study was performed four times. The relative test-line intensities were then quantified using a custom MATLAB script developed by our lab, and the results are shown in **Fig. 7**. These results demonstrate the ability of our nanzyme signal enhanced assay to consistently detect for N-protein in serum down to 0.1 ng/mL. This is at least a 10-fold improvement over the 1 ng/mL result initially seen in the unenhanced LFA. This current detection limit falls within the physiologically relevant range of serum N-protein concentrations reported for SARS-CoV-2.⁵⁻⁷

Compared to current commercially available LFAs that rely on the high N-protein concentrations in nasal and nasopharyngeal fluids, our device can detect for the lower N-protein concentrations in serum. This makes our device compatible with serum, whose collection is more consistent and less prone to user error than using nasal or nasopharyngeal swabs.

Additionally, as the signal enhancement step requires only a single button push from the user, our device is able to achieve this improved sensitivity without the addition of any liquid and test strip handling steps or electronic devices. Comparing the results of our device to a recently developed smartphone-based microfluidic device, we achieve the same detection limit of 0.1 ng/mL despite our device not having any electronic components.¹⁴

Finally, with slight modifications, our signal enhanced assay would be suitable for the detection of N-protein in swab-based samples and could also be adapted for the detection of SARS-CoV-2 spike protein or other antigen targets.

While our device has a more complex construction than the conventional LFA, the casing can still be mass produced using injection molding processes and the test strips can be created

using existing LFA diagnostic manufacturing infrastructure. Moreover, compared to other approaches to improve sensitivity such as the integration of electronic readers, our device is much less complex, making it easier to scale-up production and be more affordable to the end user.²⁵ The steps for operation are also not much more difficult than the conventional LFA, requiring just an additional press of a button.

3.2 Cross-reactivity tests with MERS-CoV and HCoV-229E N-proteins

To evaluate the cross-reactivity of our device, we ran our assay with N-proteins from the SARS-CoV-2, MERS-CoV, and HCoV-229E viruses at 1.0 ng/mL in human serum. Each test was performed three times. The unenhanced and enhanced LFA results, as well as a MATLAB analysis of the test line intensities, are provided in **Fig. 8**. The results show clear detection of the SARS-CoV-2 N-protein and no cross-reactivity with the MERS-CoV and HCoV-229E N-proteins. While future sensitivity and specificity tests would be required before commercialization, the success of the cross-reactivity tests provides the initial steps towards functional evaluation of our device.

Conclusions

In summary, we have developed a nanzyme signal enhanced LFA for the improved detection of the N-protein of SARS-CoV-2 in serum. An innovative 3D printable casing was designed, which stored all assay components including the LFA test strip, dehydrated signal enhancement reagents, and a sealed chamber with stored liquid enhancement buffer. Our paper-based device was able to detect N-protein in undiluted serum in 40 min at concentrations as low as 0.1 ng/mL, which was at least a 10-fold improvement over the conventional LFA. Moreover, with this all-in-one device, only one simple step of pushing a single button is needed for the signal enhancement to occur after the LFA detection step. The development of devices that have the ability to detect for SARS-CoV-2 antigen biomarkers

with improved sensitivity, while maintaining a user-friendly design and scalable manufacturing, is vital to increasing the frequency in screening asymptomatic individuals. This has the potential to significantly improve the response to the COVID-19 pandemic by effectively detecting patients at their early stages of infection and allowing for effective treatment and quarantining procedures to be implemented.

Author Contributions

Conceptualization: DWB, JTT, MJR, CMC, YD, RS, BMW, DTK. Investigation: DWB, JTT, MJR, CMC, JL, FDN. Methodology: DWB, JTT, MJR, CMC. Formal analysis: DWB, JTT, MJR, CMC, JL, FDN, DTK. Validation: DWB, JTT, MJR, CMC. Writing - original draft: DWB, JTT, MJR, CMC, DTK. Writing - review & editing: JL, FDN, YD, RS, BMW. Funding acquisition: RS, DTK. Project administration: DWB, FDN, DTK. Supervision: DTK. Resources: BMW, DTK.

Conflicts of interest

D.T. Kamei, D.W. Bradbury, R. Sun, Y. Du, B.M. Wu, J.T. Trinh, M.J. Ryan, and C.M. Cantu are co-inventors on a patent application on this technology filed through the University of California, Los Angeles.

Acknowledgements

This project was supported by the UCLA Technology Development Group & School of Medicine and by the National Science Foundation (NSF) Grant 1707194. C.M. Cantu would like to thank the National Institutes of Health (NIH) UCLA Maximizing Student Development (MSD) Program R25GM055052 for her research scholarship.

References

- 1 P. Pokhrel, C. Hu and H. Mao, *ACS sensors*, 2020, **5**, 2283–2296.
- 2 D. Wu, T. Wu, Q. Liu and Z. Yang, *International Journal of Infectious Diseases*, 2020, **94**, 44–48.
- 3 Z. Bai, Y. Cao, W. Liu and J. Li, *Viruses* 2021, Vol. 13, Page 1115, 2021, **13**, 1115.
- 4 S. Kammila, D. Das, P. K. Bhatnagar, H. H. Sunwoo, G. Zayas-Zamora, M. King and M. R. Suresh, *Journal of Virological Methods*, 2008, **152**, 77–84.
- 5 X.-Y. Che, W. Hao, Y. Wang, B. Di, K. Yin, Y.-C. Xu, C.-S. Feng, Z.-Y. Wan, V. C. C. Cheng and K.-Y. Yuen, *Emerging Infectious Diseases*, 2004, **10**, 1947–1949.
- 6 D. Shan, J. M. Johnson, S. C. Fernandes, H. Suib, S. Hwang, D. Wuelfing, M. Mendes, M. Holdridge, E. M. Burke, K. Beauregard, Y. Zhang, M. Cleary, S. Xu, X. Yao, P. P. Patel, T. Plavina, D. H. Wilson, L. Chang, K. M. Kaiser, J. Nattermann, S. v. Schmidt, E. Latz, K. Hrusovsky, D. Mattoon and A. J. Ball, *Nature Communications*, 2021, **12**, 1931.
- 7 T. Li, L. Wang, H. Wang, X. Li, S. Zhang, Y. Xu and W. Wei, *Frontiers in Cellular and Infection Microbiology*, 2020, **10**, 470.
- 8 V. M. Corman, V. C. Haage, T. Bleicker, M. L. Schmidt, B. Mühlmann, M. Zuchowski, W. K. Jo, P. Tscheak, E. Möncke-Buchner, M. A. Müller, A. Krumbholz, J. F. Drexler and C. Drosten, *The Lancet Microbe*, 2021, **2**, e311–e319.
- 9 M. Linares, R. Perez-Tanoira, A. Carrero, J. Romanyk, F. Perez-Garcia, P. Comez-Herruz, T. Arroyo and J. Cuadros, *Journal of Clinical Virology*, 2020, **133**, 104659.
- 10 I. Santiago, *ChemBioChem*, 2020, **21**, 2880–2889.
- 11 In Vitro Diagnostics EUAs - Antigen Diagnostic Tests for SARS-CoV-2, <https://www.fda.gov/medical-devices/coronavirus-disease-2019-covid-19-emergency-use-authorizations-medical-devices/in-vitro-diagnostic-euas-antigen-diagnostic-tests-sars-cov-2>, (accessed July 9, 2021).
- 12 G. Lippi, A.-M. Simundic and M. Plebani, *Clinical Chemistry and Laboratory Medicine (CCLM)*, 2020, **58**, 1070–1076.
- 13 D. Basso, A. Aita, F. Navaglia, E. Franchin, P. Fioretto, S. Moz, D. Bozzato, C.-F. Zambon, B. Martin, C. Dal Prà, A. Crisanti and M. Plebani, *Clinical Chemistry and Laboratory Medicine (CCLM)*, 2020, **58**, 1579–1586.
- 14 J. Li and P. B. Lillehoj, *ACS Sensors*, 2021, **6**, 1270–1278.
- 15 D. Liu, C. Ju, C. Han, R. Shi, X. Chen, D. Duan, J. Yan and X. Yan, *Biosensors and Bioelectronics*, 2021, **173**, 112817.
- 16 D. W. Bradbury, M. Azimi, A. J. Diaz, A. A. Pan, C. H. Falktoft, B. M. Wu and D. T. Kamei, *Analytical Chemistry*, 2019, **91**, 12046–12054.
- 17 Q. Shen, H. Liang, J. Tian, C. Zhou, A. Gao, D. Wang, J. Ni and D. Cui, *Nano Biomedicine and Engineering*, 2020, **12**, 325–330.
- 18 J. Tian, K. Wang, Y. Liu, H. Liang, X. Li and D. Cui, *Nano Biomedicine and Engineering*, 2020, **12**, 306–310.
- 19 X. Liu, K. Wang, B. Cao, L. Shen, X. Ke, D. Cui, C. Zhong and W. Li, *Analytical chemistry*, 2021, **93**, 3626–3634.
- 20 J. Yang, K. Wang, H. Xu, W. Yan, Q. Jin and D. Cui, *Talanta*, 2019, **202**, 96–110.
- 21 X. Zhang, D. Li, C. Wang, X. Zhi, C. Zhang, K. Wang and D. Cui, *Journal of biomedical nanotechnology*, 2012, **8**, 372–379.
- 22 B. G. Andryukov, *AIMS Microbiology*, 2020, **6**, 280.
- 23 Z. Gao, H. Ye, D. Tang, J. Tao, S. Habibi, A. Minerick, D. Tang and X. Xia, *Nano Letters*, 2017, **17**, 5572–5579.
- 24 E. Jue, C. D. Yamanishi, R. Y. T. Chiu, B. M. Wu and D. T. Kamei, *Biotechnology and Bioengineering*, 2014, **111**, 2499–2507.
- 25 T. Peng, X. Liu, L. G. Adams, G. Agarwal, B. Akey, J. Cirillo, V. Deckert, S. Delfan, E. Fry, Z. Han, P. Hemmer, G. Kattawar, M. Kim, M. C. Lee, C. Lu, J. Mogford, R. Nessler, B. Neuman, X. Nie, J. Pan, J. Pryor, N. Rajil, Y. Shih, A. Sokolov, A. Svidzinsky, D. Wang, Z. Yi, A. Zheltikov and M. Scully, *Applied Physics Letters*, 2020, **117**, 2–5.